CHARACTERISATION, DISPERSION AND ELECTROSTATIC HAZARDS OF LIQUID HYDROGEN FOR THE PRESLHY PROJECT

Hall, J.E., Hooker, P., Lyons, K., Coldrick, S., Atkinson, G., Tooke, A., Royle, M. and Willoughby, D.
Science Division, Health and Safety Executive, Harpur Hill, Buxton, SK179JN, UK,
Jonathan.Hall@hse.gov.uk

ABSTRACT

Liquid hydrogen has the potential to form part of the energy strategy in the future due to the need to decarbonise and replace fossil fuels and therefore could see widespread use. Adoption of LH2 means that the associated hazards need to be understood and managed. In recognition of this, the European Union Fuel Cells and Hydrogen Joint Undertaking co-funded project PRESLHY undertook pre-normative research for the safe use of cryogenic liquid hydrogen in non-industrial settings. Several key scenarios were identified as knowledge gaps, and both theoretical and experimental studies were conducted to provide insight into these scenarios. This included experiments studying the evolution/dispersion of a hydrogen cloud following a liquid release and the generation of electrostatic charges in hydrogen plumes and pipework, each of which are described and discussed. In addition, assessment of the physical phase of the hydrogen flow within the pipework (i.e. liquid, gas or two phase) was investigated. The objectives, experimental set up and result summary are provided. Data generated from these experiments is to be used to generate and validate theoretical models and ultimately contribute to the development of regulations, codes, and standards for the storage, handling and use of liquid hydrogen.

NOMENCLATURE

PRESLHY	Pre-normative research for safe use of liquid hydrogen
FCH JU	The fuel cells and hydrogen joint undertaking
HSE SD	UK Health and Safety Executive, Science Division
LH_2	Liquid (cryogenic) hydrogen
N_2	Gaseous nitrogen
NREL	US National Renewable Energy Laboratory
H_2	Gaseous hydrogen
ppm	Parts per million
vol%	Volume percent
LEL	Lower explosive limit

1.0 INTRODUCTION

This paper summarises the set up and conclusions from a series of experiments investigating the release, dispersion and electrostatic properties of releases of LH_2. The experiments investigate release, dispersion and mixing phenomena of LH_2 and form part of Work Packages 3 and 4 of the PRESLHY project. All work was undertaken at a bespoke LH_2 facility at HSE, Science Division, Buxton, UK site.

1.1 Project background, history and knowledge gaps

"PRESLHY" is a European Union FCH JU 2.0 co-funded research and innovation activity (Project ID 779613), addressing pre-normative work for the safe use of liquid (cryogenic) hydrogen as an energy carrier. The main project objectives are to identify safety critical areas where knowledge gaps exist and specific national standards are needed. Based on the research studies, those gaps will be closed by developing and validating new appropriate models and engineering correlations; in turn, these will help to evaluate efficient hazard mitigation concepts including consistent safety distance rules for LH_2 based technologies [1].

The work performed by HSE SD for PRESLHY is a direct continuation of LH_2 research undertaken by HSE since 2010. Previous representative HSE studies have related to the production of an LH_2

'positions paper' [2] and an internally funded research programme investigating the unignited [3] and ignited [4] hazards and phenomena from an LH_2 road tanker transfer hose rupture. Key knowledge gaps investigated in this new study include: the ability for rainout (which is where droplets of LH_2, or condensed components of air, fall from the jet or plume onto the ground) to occur during various release conditions; full source-term characterisation including mass flow; flammable extent of different sized releases and the electrostatic hazard potential within pipework and in a release cloud.

1.2 Theory

As described in PRESLHY deliverable D3.1 [5], there are several factors of LH_2 that make dispersion modelling challenging, which are mostly introduced by the extreme low temperatures ~20 K. An additional factor is that LH_2 release can be characterised by two distinct regions; the 'near-field' where the air is subjected to cryogenic temperatures and the H_2 behaves as a momentum dominated jet, and the 'far-field' where the H_2 has been warmed and behaves as a buoyancy/wind driven vapour cloud.

In the near-field region, H_2 also exists in multiple phases (liquid, gas, or two phase) each phase of which interacts differently with the air in which it comes into contact; a typical response is that water vapour present in the near-field condenses and freezes and the air also can undergo phase changes (e.g. solidification of oxygen/nitrogen). This leads to the potential for the formation of rainout. Rainout was proposed to be affected by elevation of release (relative to the ground) and so this has been an area included in this study, as has pooling of the products of rainout.

By way of comparison, the far-field is characterised by gaseous H_2 interacting with the water vapour in the air forming a visible mist. While still cold, the temperature is typically above cryogenic conditions so phase changes of other components of air are unlikely. In combination, these result in complicated multiphase, multi-component mixing and flow of material throughout the plane of the release.

In addition, previous studies have shown that the release of LH_2 into the atmosphere can produce electrostatically charged clouds [6]. Charged clouds with a high charge density could potentially result in electrostatic discharges that may cause ignition of flammable regions within the cloud. Whilst normal earthing practices can be effective to avoid spark discharges from pipework and equipment, ignition due to charged clouds was identified as an area that warranted further investigation within this study.

Electrostatic charging of a hydrogen jet is achieved as the liquid flows along pipework or is ejected from the nozzle. This charging becomes evident as a streaming current as the jet leaves the nozzle: for all liquids, streaming current can be calculated from the charge density multiplied by the liquid flow rate. For flow along the pipe, studies suggest that liquids take some distance to fully charge [7] and the streaming current at distance, L, along the pipe can be expressed as a proportion of the maximum streaming current, I_∞, using the relationship shown in Equation 1:

$$I_L = I_\infty\left(1 - e^{\left(-\frac{L}{v\varepsilon_0\varepsilon_r\rho}\right)}\right) \qquad \text{(Eq. 1)}$$

where: I_L - streaming current after travelling a distance, L, along the pipe, A; I_∞ - streaming current after travelling an infinite distance along the pipe, A; v - velocity of liquid in the pipe, $m{\cdot}s^{-1}$; L - distance along the pipe, m; ε_0 - permittivity of air, ca. $8.85x10^{-12}$ $F{\cdot}m^{-1}$; ε_r - relative permittivity of LH_2, R 1.23 [8]; ρ - resistivity of LH_2, $1x10^{15}$ $\Omega{\cdot}m$ [6].

This formula indicates that LH_2, having a very high resistivity, would require a very long length to become fully charged. Therefore, LH_2 would not be expected to accumulate significant charge in the relatively short length of pipe used in the experiments and charging currents were predicted in be in the order of pA. In these experiments, the wall current (i.e. the degree of charging taking place within an isolated pipe section) was measured to test if this prediction would persist during the scenario of an uncontrolled LH_2 leak. Further charging occurs as the liquid leaves the pipe forming droplets and additional charging may result from droplet and solid particle interactions within the jet.

Estimates of charge density within the ejected jet were also planned to be made by measuring the electric field in the vicinity of the LH_2 release point by use of a field meter and Faraday pail. Knowledge of the electric field allows the charge density to be estimated via Equation 2and hence an assessment made of the risk of ignition from an electrostatic discharge.

$$\sigma = \frac{2\varepsilon_0 \varepsilon_r E}{R} \qquad \text{(Eq. 2)}$$

where: σ - charge density within the cloud (C m^{-3}), E - measured electric field (V m^{-1}), R - radius of the cage (0.125 m), ε_0 - permittivity of air (ca. 8.85 x 10^{-12} F m^{-1}), ε_r - relative permittivity of the cloud, (approx. = 1)

2.0 EXPERIMENTAL SET UP

This section provides a summary of the test facility and experimental set up developed for the PRESLHY project. A more complete description of the set up can be found in the PRESLHY deliverable reports [9] and [10] respectively.

In general, characterisation of the dispersion from releases was measured in terms of H_2 concentration and temperature by a combination of thermocouples and gas sensors. Other attributes such as pressure, mass flow rate and temperature were measured in the supporting pipework to characterise the source term. To meet the trial objectives, a series of 25 unignited LH_2 releases were carried out through 6 mm, 12 mm, and 25.4 mm nozzles with an indicated tanker delivery pressure of 100 kPa or 500 kPa and variation in release heights of 0.5 m or 1.5 m.

Electrostatic charging experiments were designed to measure two distinct modes of charging: (i) the charged cloud generated by a jet of H_2, which may be liquid, gaseous or two-phase; and (ii) the charging due to charge separation near to the LH_2/pipe interface (monitored via the wall current from an electrically isolated section of pipework). In order to measure the charged cloud formed by the H_2 jet, a series of seven experiments were conducted, whereby, LH_2 was released through the path of a field meter or Faraday cage. Simultaneously, wall current measurements were made using an electrometer connected to an electrically isolated section of pipework prior to the release point. The wall current measurements were taken during five of the seven electrostatic trials as well as all of the 25 rainout experiments (WP3). For a full assessment of the electrostatic measurement methods that were considered and the rationale for adopting those that were used, see PRESLHY D4.1 [11].

2.1 Hydrogen release test facility – General Arrangement

The experiments were conducted using the HSE LH_2 release facility, located on a 32 m diameter concrete pad. The experiments consisted of four main components shown in Figures 1a and b: the LH_2 release station, the tanker and vent stack, the near-field sensor array, and the far-field sensor stands.

The LH_2 was supplied by Air Liquide where control of the pressure and conditioning of the LH_2 inside the tanker was achieved through venting the ullage of H_2 to moderate the pressure and liquid temperature (LH_2 could also be passed into a heat exchanger underneath the tanker to raise the pressure). A 1.2 MPa bursting disk protected the tanker against overpressurisation. Pressure was recorded for each trial from the dial gauge on the tanker. One type T thermocouple was installed on the lower face of the vent stack exit and N_2 and H_2 gas cylinders were used to purge the release pipework of air prior to the introduction of any LH_2.

Figure 1a (left): Overhead image of test site: LH_2 release station (green), tanker and vent stack (yellow), near-field array (blue) and the far-field stands (red). Figure 1b (right): Image of the LH_2 tanker, vent stack and purging station.

2.2 Instrumentation

Multiple types of instrumentation were deployed during WP3 and WP4 experiments, separated into three groups, 'near-field', 'far-field' and 'electrostatics'.

2.2.1 Gas concentration and temperature (near-field)

To capture the H_2 concentration profile of the jet formed by a release of LH_2, an array supporting 31 sampling tube lines and 24 type T thermocouples was placed downstream of the release point, Figure 2a. Each thermocouple was collocated with a sampling line and each sampling line was linked to a Xensor XEN-TCG-3880 thermal conductivity sensors (supplied by NREL). Prior to LH_2 release, the release station and near-field array were oriented with the prevailing wind direction. Releases were carried out at 0.5 m and 1.5 m above the ground and varied in release orientation, i.e. upward, downward and horizontally.

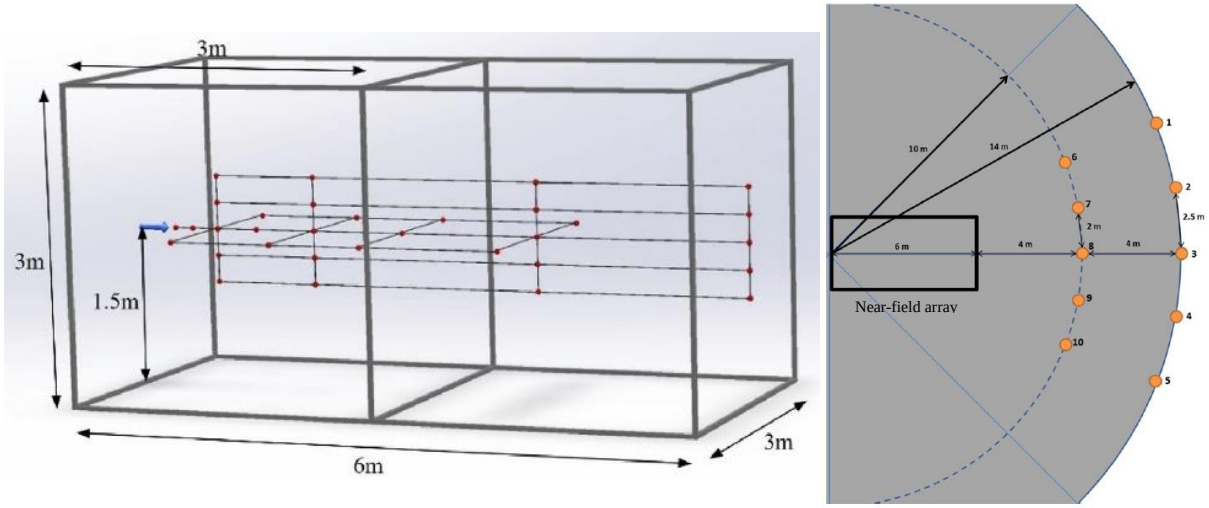

Figure 2a (left): Near-field sensor array (→ LH_2 release point, • H_2 sampling points with collocated thermocouples [12]). Figure 2b (right): Far-field gas sensor array. For complete sensor location measurements see D3.6 [9].

2.2.2 Gas concentration and temperature (far-field)

To observe the downstream plume behavior, 10 mobile stands, each with three Dräger Xam 5000 personal gas detection devices and collocated type T thermocouples, were arranged in the expected

dispersion path, Figure 2b. The Dräger devices each contained four sensors: H_2 ppm, H_2 vol%, H_2 %LEL and oxygen depletion.

2.2.3 Electrostatics

Wall current was measured using a Keithley 6514 electrometer connected to a 0.5 m section of electrically isolated pipework achieved using PTFE gaskets and bolt sleeves, phenolic insulation and a Mylar wrap. Figure 3a shows the section of electrically isolated pipework and the connection to the electrometer. Resistance to ground measurements were taken with a RT-1000 resistance meter periodically during the test days. Two field meters were used throughout the experimental series in order to measure the charge generated by the LH_2 cloud; firstly an IDB Systems ID107HS static field meter was mounted in line with the stream of the jet, and secondly an IDB Systems rugged field meter ID-939R used in conjunction with a Faraday pail with a diameter of 0.25 m. This setup is shown in Figure 3b.

Figure 3a (left): 0.5 m electrically isolated pipework section measuring wall current. Figure 3b (right): A field meter with a Faraday pail measuring the charge generated by the cloud.

2.2.4 Release station

The release station encompassed the pipework and valves required to operate the system remotely as well as instrumentation to characterise the flow of LH_2 and a weather station. For these tests this consisted of an electrically isolated pipe section, a valve section and a flexible hose with a nominal pipework bore of 25.4 mm. The instrumentation consisted of two 1 MPa pressure transducers with heat exchanging pig tails, four type T thermocouples and a Micro Motion CFM100 coriolis mass flow meter with an Elite 5700 transmitter. Figure 4 shows the release station post trial.

The mass flow meter was modified by the manufacturer in collaboration with HSE SD to facilitate operation at temperatures of 20 K. The modifications made, listed below, were based on another organisation's previous experience gained with liquid helium [13].

- the integrated temperature sensor (PT100) used for temperature correction of the modulus of elasticity for the flow tubes (required for density measurement) was disabled as it cannot survive below 73 K (the modulus correction was fixed at 20 K);
- the wire gauge of the strain gauge connections to the flow tubes were increased as repeated temperature cycling to ~20 K is known to cause failure of this component; and
- the casing around the flow tubes was evacuated, rather than nitrogen filled to avoid freezing which would affect the sensing coils/magnets and flow tubes. The vacuum also serves as an additional benefit as it will thermally insulate the flow from the body of the meter.

The mass flow meter provides three outputs; mass flow, drive gain and density (the density measurement accuracy relies on an assumption of 20 K to be accurate).

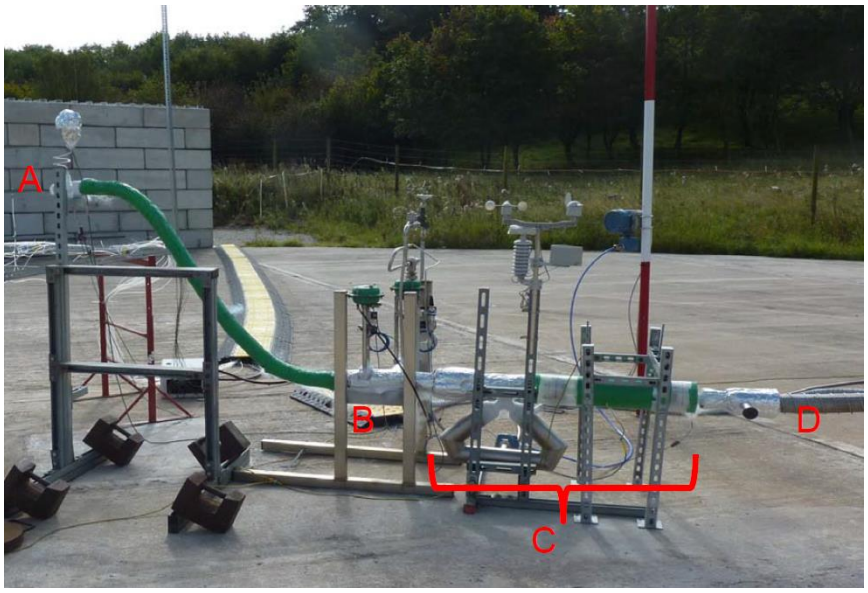

Figure 4: Release station; A: nozzle, B: final release valve, C: measurement section (electrostatics and mass flow/density), D: Vacuum insulated pipe to tanker.

3.0 RESULTS

A series of 25 unignited LH_2 releases were carried out through 6, 12, and 25.4 mm nozzles with an indicated tanker pressure of 100 or 500 kPa and release heights of 0.5 or 1.5 m. A selection of representative results is given below with full details being given in D3.6 [9] and D4.6 [10].

3.1 Release phenomena - Rainout

One of the main objectives of the trials was to establish the propensity for droplets of LH_2 to form and fall to the ground from elevated LH_2 releases.

For un-impinged elevated releases, no evidence of rainout was observed during the release phase, however, in some circumstances, condensates did occur on closure of the release valve, Figure 5a. No pool formed from this type of droplet formation as the droplets evaporated rapidly on contact with the ground. It was noted that for all releases, either through 12 mm or 6 mm orifices, white cone deposits at the release point were consistently formed. Evidence of the formations altering the jet was also observed, including an example of the jet becoming two separate streams, shown in Figure 5b. These formations would form and then subsequently break off periodically throughout a release.

Figure 5a (left): Droplet rainout occurring immediately after flow is stopped and jet momentum is lost. Figure 5b (right): Solid build-up on the release nozzle causing the jet to split.

When conducting high pressure releases (500 kPa tanker pressure) it was observed that the LH_2 jet interacted directly with the closest sampling lines of the near-field sensors. This led to large solid deposits to form, blocking the sampling tubes and distorting the jet at that location, Figure 6. Periodically, part of this formation would dislodge and fall to the floor, where it appeared to sublime.

Figure 6a (left): Pre-trial view of the nozzle and near-field sensors. Figure 6b (right): Solid deposit forming on the nearest sample line during 500 kPa release.

Pools did not form during the majority of the trials, with the exception of the releases oriented vertically downwards, where pools of approximately 1.7 m diameter formed. This was evidenced by frost marks on the concrete following the tests and the video captured during the trials (although visibility was heavily obscured due to the formation of mist).

The possibility of rainout occurring at the vent stack exit during a venting operation was also explored; however, the temperature did not fall below approximately 83 K throughout the entire experimental series including long periods of venting indicating no LH_2 exited the vent stack.

3.2 Mass flow and phase

The mass flow meter only provided reliable data when the flow is single phase. When flashing[1] occurs prior to the meter, the results became unreliable and tended to under-read flowrate. It was found that variation of the 'drive gain' of the meter (the power required to oscillate the meter tubes to their resonant frequency) provided a means of identifying the phase of the flow (where high drive gain indicated gaseous or two-phase flow and steady low drive gain indicated liquid flow, i.e. a denser fluid).

Mass flows readings for 6 and 12 mm nozzles at 500 kPa are known with confidence as drive gain and density indicates liquid flow throughout the meter. In other cases (100 kPa and/or open pipe) the mass flow meter encountered 2-phase flow with a high void fraction and did not give reliable outputs. Where 2 phase flow was observed, mass flow was derived from the pipework pressure measurements. It was found that one source condition could not be measured directly or derived, (driving pressure of 100 kPa and a nozzle diameter of 6 mm). Under these conditions, the flow through the meter became predominantly gaseous and the subsequent flow rate/pipework pressure drop was too low for the flow meter/pressure transducers to resolve. A summary of the measured and derived mass flow data is given in Table 1.

The mass flow in previous work on solid accumulation [3, 4] used much of the same equipment and the PRESLHY data can be used to estimate the flow rate in these experiments at approximately 135 g/s. A detailed description of the methods used to interpret flow rate and density measurements is given in PRESLHY deliverable D3.6 [9].

[1] Flashing refers to the process of the LH_2 changing from a liquid to a vapour or gas.

Table 1. Summary of mass flow rates for the various test configurations

Pressure (kPa)	Nozzle diameter (mm)	Mass flow (g/s)	Flow conditions
500	6.0	90-100	Liquid up to nozzle
500	12.0	265	Liquid up to nozzle
500	25.4 (open pipe)	298*	Flashing prior to the meter
100	6.0	Not measurable	Flashing prior to the meter
100	12.0	104-107*	Flashing prior to the meter
100	25.4 (open pipe)	135-144*	Flashing prior to the meter
*Mass flow values reported in these instances are derived from pressure measurements rather than taken from the mass flow meter			

3.3 Gas cloud concentration and temperature profile

In the near-field array, concentration and temperature measurements were achieved by averaging each point during a steady state period of a release; this allowed transient effects of the dynamic wind conditions to be mitigated and comparisons made between tests.

By way of example, Figure 7a and b compare the average H_2 concentrations across the near-field array at 0.5 m above the ground for a 12 mm nozzle and tanker pressures of 100 and 500 kPa respectively. It can be seen that Figure 7b shows lower than expected concentrations along the centerline close to the release point, in comparison with Figure 7a. This is thought to have been caused by solid deposits which developed on the sampling lines during the 'higher pressure' trials, effectively blocking the sensor, as seen in Figure 6b.

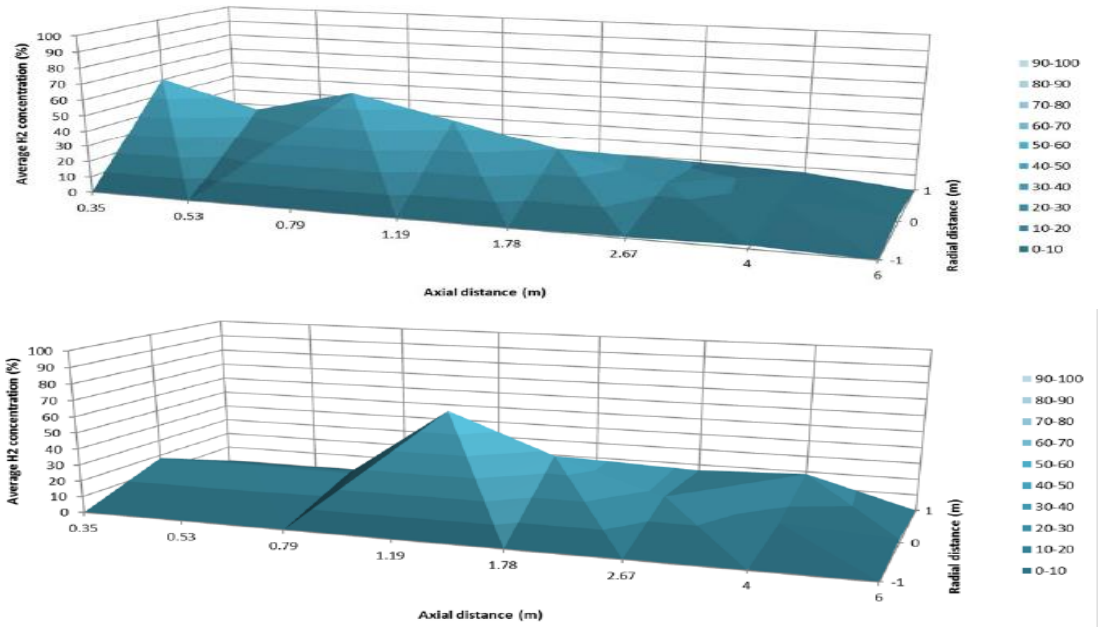

Figure 7a (top): A near-field time averaged gas concentration profile for 12 mm, 100 kPa. Figure 7b (bottom): A near-field time averaged gas concentration profile for 12 mm, 500 kPa

As detailed above, the near-field H_2 concentration sensors were supplemented with 24 type T thermocouples and for each test, the minimum temperature and maximum gas concentration at each collocated point were plotted. This is shown in Figure 8. Except for a small number of outliers, the data show that the temperature is inversely proportion to the H_2 concentration. This relationship is due to be examined further as a future part of the PRESLHY project aimed at predicting the concentration of H_2 based on temperature measurements and humidity [14].

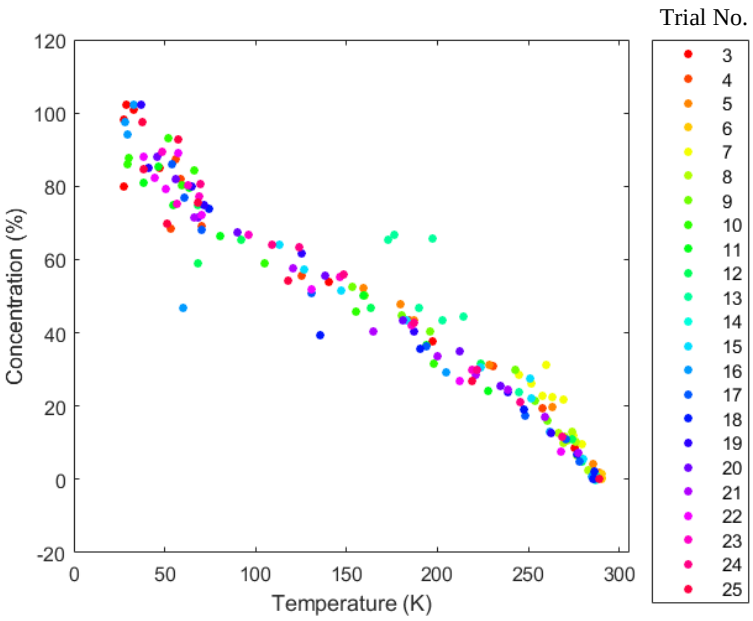

Figure 8: Graph showing the minimum temperature and maximum near-field H_2 concentration at points along the centerline, coloured by trial.

Due to the response time (20 s) of the far-field sensors, transient pockets of H_2 could not be reported in real time without significant interpretation and assumption. However, the sensors did provide a means of assessing qualitatively whether flammable concentrations of H_2 are present at close to ground level for the various releases (which is a key parameter for hazardous area classification). Results showed that >100% LEL H_2 was present at 14 m downwind of the release point, 1.5 m above the ground for all but the 6 mm releases (which showed >50% LEL at the same distance).

3.4 Electrical field strength of a multiphase jet

The baseline electric field strength measured during LH_2 releases was low. Some occasional short duration increases were observed at ca. 100 - 200 V m^{-1} although these excursions were of the same order of magnitude as the common background atmospheric electric fields, (as shown in Figure 9). Experimentation suggested that these excursions were associated with initial purging of air from the end of the release nozzle, or from the accumulation, and subsequent break-off, of solids at the nozzle.

The small electric fields indicate that ignition by lightning type discharges from the cloud will not occur as very high fields (hundreds of kV m^{-1}) are required for this [15]. The electric field strength present also suggests that the initiation of corona discharges capable of causing ignition is also unlikely [16, 17]. One area of future study is the potential for charged solid material to break off and enter the plume giving rise to an electrostatic discharge path.

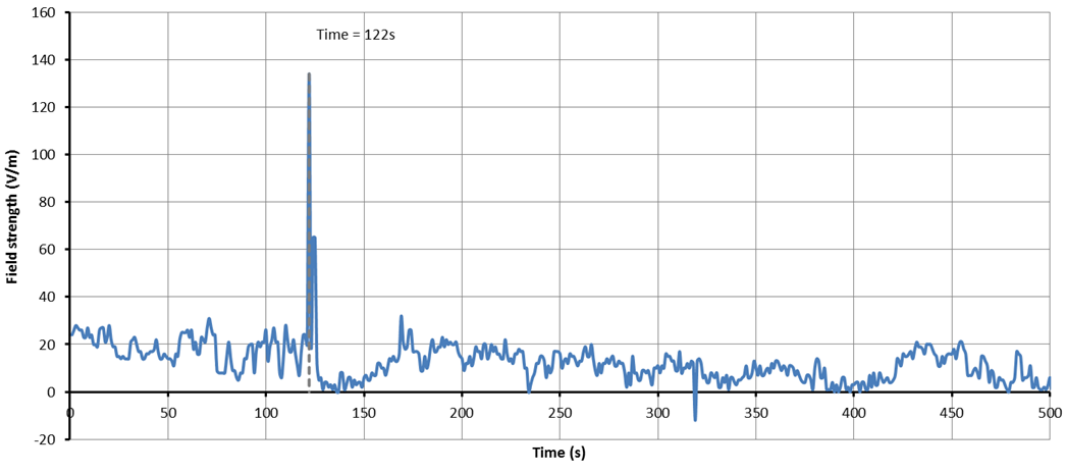

Figure 9: Electric field measurement from 500 kPa tanker pressure and a 6 mm nozzle.

3.5 Wall current

Generally, the wall currents measured were very low, typically considerably less than $50x10^{-9}$ A. Larger wall currents were observed when two phase flow was suspected to be occurring as shown in Figure 10. Currents exceeding the selected range of the electrometer occurred in some instances; the largest wall current detected exceeded $2.8x10^{-6}$ A (i.e. 2.8 µA). This increase in charging is typical of two-phase systems (e.g. pneumatic conveying of solids [15] or flow of two-phase liquids [18]) where triboelectric effects and charge retention on the solid become more prevalent.

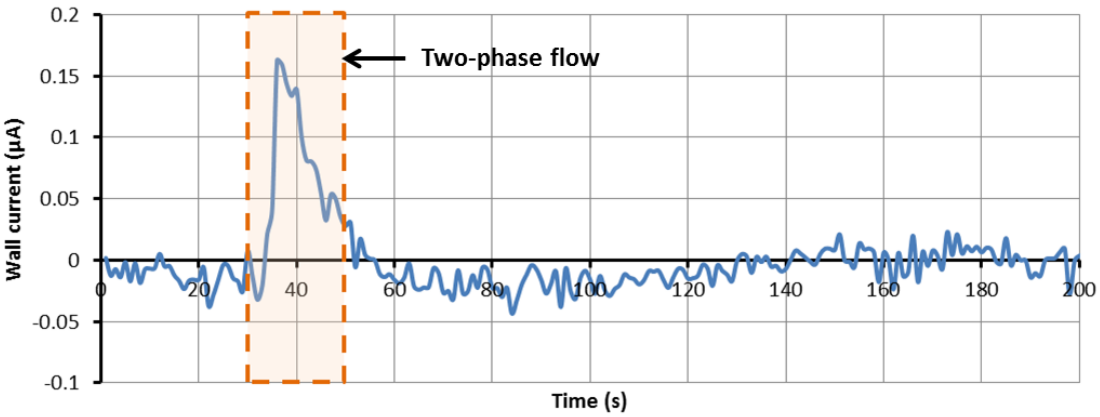

Figure 10: Wall current measurement from 500 kPa tanker pressure and a 25 mm nozzle

Although increased charging during two-phase flow was observed, this is not considered to be an issue as standard earthing practices, providing a resistance to earth of less than 10 ohms for metallic items, will maintain electrical potential on pipelines and plant below hazardous levels.

4.0 CONCLUSIONS

A series of 25 large scale LH_2 releases were carried out through 6 mm, 12 mm and 25.4 mm nozzles in various orientations with an indicated tanker pressure of 100 or 500 kPa and release heights of 0.5 or 1.5 m. Pipework temperature, pressure and mass flow measurements enabled a characterisation of the release and downstream temperature whilst concentration sensors enabled the analysis of the subsequent dispersion.

4.1 Rainout, pooling and solid deposition

Rainout did not occur during established flows regardless of release orientation. However, dropout of an unconfirmed composition did occur from a 500 kPa release once the flow was stopped indicating that rainout may occur when jet momentum or upstream driving is suddenly lowered. Rainout cannot therefore be ruled out as a credible phenomenon for LH_2 spills, although for normal LH_2 tanker decant operations it would appear unlikely and the hazards of such an event would be minimal (i.e. minimal volumes following isolation).

Solid deposits were observed to form around the release point when ≤12 mm nozzles were used and on impingements close to the release point. In some cases, these deposits impeded measurements and affected the flow path from the nozzle. Liquid pools only formed with vertically downwards releases.

4.2 Outflow rates

Three different flow regimes were identified from the mass flow meter output: gaseous, liquid, and two-phase flow. The accuracy and reliability of the mass flow measurements was higher for gaseous or liquid flows and was only reportable for the 500 kPa releases through reduced nozzles. Two-phase flow with high void fractions caused large errors in mass flow measurement with the Coriolis meter.

Where the flow rate could not be directly measured, the flow was derived using pressure, temperature and phase information collected [9]. Typical LH_2 flow rates in these experiments was estimated at up to 144 g/s and 298 g/s for 100 kPa and 500 kPa releases respectively.

4.3 Dispersion

In depth assessment of the data collected is not included in this paper and further work is ongoing to provide a more detailed assessment of the near-field data and the intricacies of the experimental set up [12, 19]. Some preliminary basic trends were however noted:

- higher pressures and larger nozzles increase the average H_2 concentration in the near-field region, despite the mass flow meter under-predicting mass flow rates when high void fractions occurred;
- transient ignitable pockets (average H_2 concentration >LEL) were measured at 14 m downwind of the LH_2 releases through 12 mm holes or larger; and at approximately 1.5 m for the 100 kPa releases and 3 to 6 m for the 500 kPa releases; and
- the dispersion of the H_2 cloud loses momentum and becomes heavily influenced by wind, including transient localised gusts.

4.4 Electrostatic hazard potential

Low level electrostatic charging of the dispersion cloud and pipework was observed as a result of releases of LH_2, both as a result of flow through the pipe and as a result of charge retention in the cloud. Full analysis of the results is not yet complete, but preliminary results suggest that the potential for ignition by electrostatic discharges in the scenarios studied appears to be low. However, the potential for accumulations of ice and condensed air components to become charged and detached, thereby presenting an ignition risk is yet to be fully assessed.

4.5 Impacts on hydrogen safety

Rainout and the ability to form a liquid pool for releases above the ground from tanker releases appear to be unlikely to present a hazard in the vast majority of release scenarios, except those releases oriented vertically downwards. The risk of ignition from electrostatic charging of the pipework is low although hazards from solid break-off and how these solids interact within the jet or plume are yet to be fully characterised. Impinged releases were also found to form solid deposits and were seen to affect nozzle dispersion which effected the flammable extent of the dispersing cloud. The data produced for this work will help validate dispersion models, inform safety distances and has already been used to develop numerical tools [20].

ACKNOWLEDGMENTS

This project received funding from the Fuel Cells and Hydrogen 2 Joint Undertaking under the European Union's Horizon 2020 research and innovation programme under grant agreement No 779613. The HSE work programme acknowledges funding from its sponsors Shell, Lloyd's Register Foundation and Equinor and instrumentation provided by Dräger. This paper's contents, including any opinions and/or conclusions expressed, are those of the authors alone and do not necessarily reflect HSE policy. Instrumentation was also provided by the Sensor Laboratory at the National Renewable Energy Laboratory (NREL), with funding from the DOE Fuel Cell Technology Office. NREL Sensor Laboratory personnel (William Buttner and Tashi Wischmeyer) also assisted HSE in interfacing the NREL Hydrogen Wide Area Monitor to the HSE LH_2 test apparatus.

REFERENCES

1. PRESLHY, Project Overview, https://preslhy.eu/project-overview/, accessed 22/03/2021
2. Pritchard, D. K., Hazards of liquid hydrogen - positions paper, Health and Safety Executive Research Report No. RR769, 2010
3. Royle, M. and Willoughby, D., Releases of unignited liquid hydrogen, Health and Safety Executive Research Report No. RR986, 2014
4. Hall, J.E., Ignited releases of liquid hydrogen, Health and Safety Executive Research Report No. RR987, 2014
5. Venetsanos, A., Theory and Analysis of Cryogenic Hydrogen Release and Dispersion, D3.1, Pre-normative REsearch for Safe use of Liquid Hydrogen (PRESLHY), 2019
6. Cassutt, L., Biron, D. and Vonnegut, B., Electrostatic hazards associated with the transfer and storage of liquid hydrogen, Advances in Cryogenic Engineering, Vol. 7, 1962
7. Cross, J. A., Electrostatics – Principles, problems and applications, ISBN 0-85274-589-3, Adam Hilger, Bristol, 1987
8. Wolfke, M et al, On the dielectric constants of liquid and solid hydrogen, Communication No. 171c from the Physical Laboratory at Leiden, (Communicated at the meeting of September 27, 1924)
9. Lyons, K., Coldrick, S., Atkinson, G., Summary of experimental series E3.5 (Rainout) results, Deliverable 3.6, Pre-normative REsearch for Safe use of Liquid HYdrogen (PRESLHY), 2020
10. Lyons, K. and Hooker, P., Summary of experimental series E4.3 (Electrostatic Ignition) results, Deliverable 4.6, Pre-normative REsearch for Safe use of Liquid HYdrogen (PRESLHY), 2020
11. Lyons, K., Proust, C., Cirrone, D., Hooker, P., Kuznetsov, M., Coldrick, S. Theory and analysis of ignition with specific conditions related to cryogenic hydrogen. Deliverable 4.1, Pre-normative REsearch for Safe use of Liquid HYdrogen (PRESLHY), 2020
12. Buttner, W. et al, Hydrogen wide area monitoring of LH2 releases, *International Journal of Hydrogen Energy*, **46**, 2021, pp. 12497-12510
13. De Jonge, T., Pattern, T., Rivetti, A. and Serio, L., Development of a mass flowmeter based on the Coriolis acceleration for liquid, supercritical and superfluid helium, European Organization for Nuclear Research: Laboratory for Particle Physics, Divisional Report CERN LHC/2002-19, 2002
14. Cirrone, D. et al, Detailed description of novel engineering tools for LH2 safety, version 2, Deliverable 6.5, Pre-normative REsearch for Safe use of Liquid HYdrogen (PRESLHY), 2021
15. BSI. PD IEC/TS 60079-32-1:2013, Explosive atmospheres. Part 32-1: Electrostatic hazards guidance, The British Standards Institution, ISBN 978 0 580 81629 1
16. Grabarczyk, Z., Laboratory ignition of hydrogen and carbon disulphide in the atmospheric air by positive corona discharge, *Journal of Electrostatics*, **71**, 2013
17. Hooker, P. et al, Self Ignition of Hydrogen by Various Mechanisms, IChemE Symposium Series No. 156, 2011

18. Gibson, N., and Harper, D., Effect of electrification in ball valves on ignition risk in liquid pipeline systems, *Journal of Electrostatics*, **1**, 1975, pp. 339–350
19. Buttner, W. et al, Hydrogen Wide Area Monitoring of LH2 Releases at HSE for the PRESLHY Project, International Conference on Hydrogen Safety, 2021, draft submission
20. Cirrone, D. et al, Detailed description of novel engineering correlations and tools for LH2 safety, version 2, Deliverable 6.5, Pre-normative REsearch for Safe use of Liquid HYdrogen (PRESLHY), 2021